A New Eddy Current Model for Magnetic Bearing Control System Design [1]

Joseph J. Feeley and Daniel J. Ahlstrom
Department of Electrical Engineering
Microelectronics Research Center
NASA Space Engineering Research Center
University of Idaho
Moscow, Idaho 83843

Abstract - **This paper describes a new VLSI-based controller for the implementation of a Linear-Quadratic-Gaussian (LQG) theory-based control system. Use of the controller is demonstrated by design of a controller for a magnetic bearing and its performance is evaluated by computer simulation.**

1 Introduction

Magnetic levitation is being used in an increasing number of applications to support rotating or reciprocating shafts. In this setting, the assemblage of power supplies, control circuits, actuator coils, pole-pieces, amplifiers, and position sensors is termed a magnetic bearing. The control of magnetic bearings is discussed in [1] and the references cited therein. Traditional control system design studies require, first of all, a simple and accurate model of the system to be controlled. The lack of such a model for magnetic actuators containing significant eddy currents has hampered recent control system design efforts [1, 2]. The purpose of this paper is to introduce a new mathematical model of eddy currents in a magnetic actuator. The model is relatively simple, appears reasonably accurate, and is convenient to use in control system design. The model is based on Maxwell's electromagnetic equations and is simplified using reasonable, ad hoc assumptions consistent with a magnetic bearing application.

A complete set of equations for the mathematical model of a magnetic bearing is presented in Section 2, and conclusions and directions of future work are discussed in Section 3.

2 Mathematical Model

For convenience in developing the mathematical model, the magnetic bearing system is separated into three subsystems: a) the magnetic actuator, b) the magnetic force production mechanism, and c) the shaft. Each of these subsystems is treated separately in the following subsections. For the sake of specificity, the model development is applied to specific magnetic bearing of interest to NASA. Figure 1 is a schematic cross-sectional view of a magnetic bearing used in a cryogenic refrigerator developed by NASA for certain space applications. The refrigerator, magnetic bearings, and associated control systems were designed and constructed by Phillips Laboratories [2].

[1]This research was supported in part by NASA under Space Engineering Research Grant NAGW-1406 and by the NSF under Research Initiation Grant MIP-9109618.

2.1.2

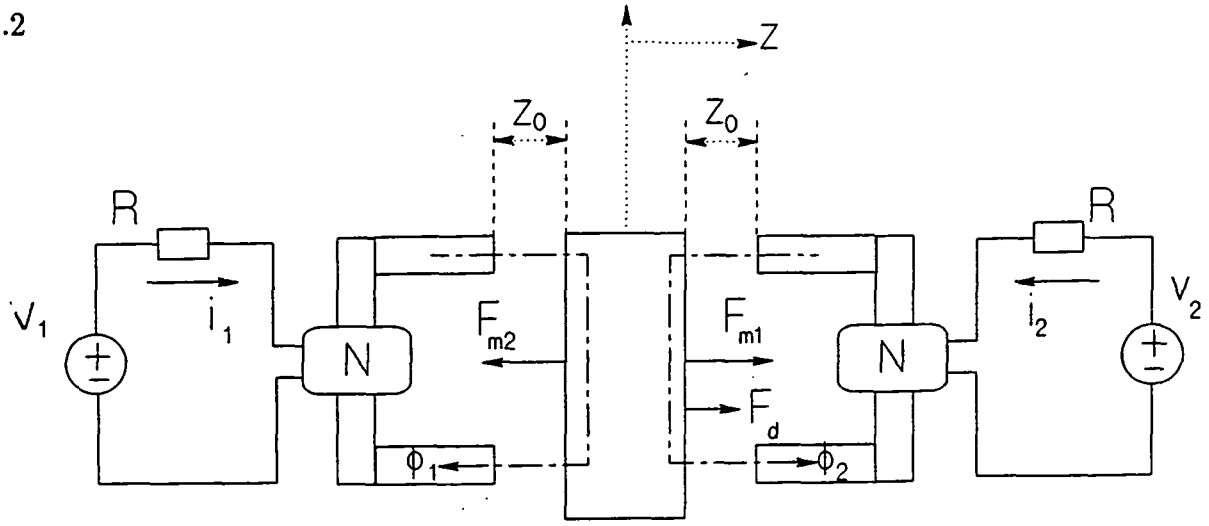

Figure 1: Cross-sectional view of magnetic bearing.

Figure 1 shows one end of a shaft centered between two diametrically opposed magnetic actuators. The actuators are activated by separate control circuits energized by voltage sources v_1 and v_2. The voltage sources are controlled in a coordinated way by a feedback controller to produce the forces required to maintain the shaft in the desired position in spite of disturbance forces. Another pair of actuators and control circuits are used to control the position of the shaft in the orthogonal plane containing the axis of the shaft. No coupling of forces between the two planes is considered and the two actuator pairs are controlled independently.

2.1 Magnetic Actuator

The purpose of this section is to develop a mathematical model relating the voltage applied to the actuator circuit to the current developed in that circuit. Applying Kirchoff's voltage law to the circuit on the left in Fig. 1 gives

$$v_1 = Ri_1 + N\frac{d\Phi_1}{dt} \tag{1}$$

where R is the resistance of the actuator circuit, i_1 is the coil current, N is the number of turns in the actuator coil, and Φ_1 is the flux in the magnetic circuit. The flux is related to the current by the magneto motive force (2) relationship

$$\Phi_1 = \frac{Ni_1}{\mathcal{R}} \tag{2}$$

where $\mathcal{R}$ is the reluctance of the magnetic circuit. Assuming the reluctance of the two air gaps is much larger than that of the magnetic material in the pole-piece, $\mathcal{R}$ can be approximated by

$$\mathcal{R} = 2\left(\frac{z_0 + z}{\mu_0 A}\right) \tag{3}$$

where $z_0 + z$ is the length of one air gap, μ_0 is the permeability of free space, and A is the area of pole-piece normal to the flux direction. Substituting (3) and (2) in (1) and carrying

out the indicated differentiation gives

$$v_1 = Ri_1 + \frac{N^2\mu_0 A}{2}\left[\frac{1}{(z_0+z)}\frac{di_1}{dt} - \frac{i_1}{(z_0+z)^2}\frac{dz}{dt}\right] \tag{4}$$

Similar analysis of the circuit on the right leads to the following expression for v_2

$$v_2 = Ri_2 + \frac{N^2\mu_0 A}{2}\left[\frac{1}{(z_0-z)}\frac{di_2}{dt} + \frac{i_2}{(z_0-z)^2}\frac{dz}{dt}\right] \tag{5}$$

Equations (4) and (5) are the desired expressions showing the relationships among control voltage, actuator current, shaft position, and shaft velocity.

2.2 Magnetic Force Production Mechanism

The purpose of this section is to develop an expression relating the current in the actuator coil to the electromagnetic force exerted on the shaft. The differential electromagnetic energy stored in an air gap as depicted in Fig. 1 is given as [3]

$$dw = \frac{1}{2}\frac{B^2 A}{\mu_0}dz \tag{6}$$

where $B = \Phi/A$ is the flux density. From Newton's second law the differential energy can also be expressed as a force acting through a differential distance

$$dw = F_m dz \tag{7}$$

Combining (6) and (7) and accounting for the presence of two air gaps, the attractive forces shown in Fig. 1 are

$$F_{m1} = \frac{B_1^2 A}{\mu_0} \tag{8}$$

and

$$F_{m2} = \frac{B_2^2 A}{\mu_0} \tag{9}$$

If the current in the actuator coil is constant, the flux it produces is constant, in both space and time, and no eddy currents are induced in the pole-piece. Further, if the majority of the mmf drop occurs in the air gaps, the mmf relationship can be used to express the flux density in terms of the coil current. The flux densities in the two magnetic circuits can then be written as

$$B_1 = \frac{\mu_0 N i_1}{2(z_0+z)} \tag{10}$$

and

$$B_2 = \frac{\mu_0 N i_2}{2(z_0 - z)} \tag{11}$$

Substituting (10) and (11) in (8) and (9) yields the usual [2] expressions for electromagnetic force in terms of the coil current and the length of the air gap

$$F_{m1} = \frac{\mu_0 N^2 A}{4}\left(\frac{i_1}{z_0 + z}\right)^2 \tag{12}$$

and

$$F_{m2} = \frac{\mu_0 N^2 A}{4}\left(\frac{i_2}{z_0 - z}\right)^2 \tag{13}$$

If, however, the current in the actuator coil changes with time, eddy currents are induced in the pole-piece. The eddy currents, in turn, produce a reactive flux in opposition to the original flux. The result of the superposition of the two effects is a reduced net flux in the pole-piece. The resultant spatial flux distribution in the pole-piece in a plane orthogonal to the flux direction is governed by the diffusion-type equation [4]

$$\frac{\partial^2 B(y,x,t)}{\partial x^2} + \frac{\partial^2 B(x,y,t)}{\partial y^2} = \sigma\mu\frac{\partial B(x,y,t)}{\partial t} \tag{14}$$

where σ and μ are the conductivity and permeability of the pole-piece material.

Equation (14) can be solved analytically for a bar whose length is long relative to its cross-sectional dimensions, $2a$ and $2b$. When excited by a sinusoidally varying actuator coil current

$$i_1(t) = I_1 \cos ax, \tag{15}$$

(10) and (15) can be used to develop the boundary conditions

$$B_1(x,y)|x \pm a, y \pm b = \frac{\mu_0 N I_1}{2(z_0 + z)} \tag{16}$$

Subject to this boundary condition, the sinusoidal steady state solution of (14) is [4]

$$B_1(x,y,z,\omega) = \frac{\mu_0 N I_1}{2(z_0 + z)}\left[\frac{\cosh(\alpha y)}{\cosh(\alpha b)} + \sum_{k=1,3,5}^{\infty} P_k \cos\left(\frac{k\pi y}{2b}\right)\cosh\left(x\sqrt{\beta_k}\right)\right] \tag{17}$$

where:

$$P_k = \frac{4\alpha^2}{k\pi\beta_k}\frac{\sin\left(\frac{k\pi}{2}\right)}{\cosh\left(a\sqrt{\beta_k}\right)} \tag{18}$$

$$\alpha = \sqrt{j\omega\sigma\mu} \tag{19}$$

and

$$\beta_k = \alpha^2 + \left(\frac{k\pi}{2b}\right)^2 \tag{20}$$

$B_1(x,y,z,\omega)$ is a complex number representing the magnitude and phase of the flux density in the pole-piece. The normalized magnitude of $B_1(x,y,z,\omega)$ is plotted in Fig. 2 with $z = 0$ and $\omega = 10$ rad/sec. The figure clearly shows the effect of eddy currents in depressing the magnitude of the flux in the central regions of the pole-piece.

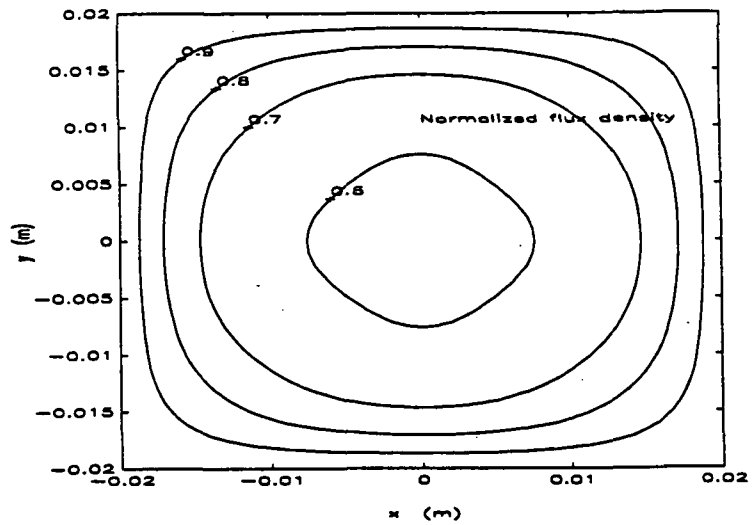

Figure 2: Contour plot of normalized magnitude of flux density.

In order to develop a simple, frequency dependent model of the force produced by the actuator current, the flux density as given by (17) is averaged over pole-piece face area yielding

$$\overline{B_1}(z,\omega) = \frac{\mu_0 N I_1}{4ab(z_0+z)}\left[\frac{1}{\alpha}tanh(\alpha b) + \left(\frac{4\alpha}{\pi}\right)^2 b \sum_{k=1,3,5}^{\infty} \frac{\sqrt{\beta_k}}{k^2\beta_k^2} tanh\left(a\sqrt{\beta_k}\right)\right] \tag{21}$$

The frequency response of $\overline{B_1}(z,\omega)$ is dominated by the $\frac{tanh(\alpha b)}{\alpha}$ term in (21), and log-magnitude and phase plots would reveal the familiar [2] high frequency roll-off of approximately 10 db/decade and 46 deg phase lag at high frequencies due to the $\sqrt{j\omega}$ factor in the α term. Substituting the spatially averaged flux density, as given by (21), for the constant flux density,B_1, in the force equation, (8), yields the following frequency dependent approximation for the magnetic force produced by a time-varying current

$$F_{m1}(z,\omega) = \frac{\mu_0 N^2}{A}\left(\frac{I_1}{z_0+z}\right)^2\left[\frac{1}{\alpha}tanh(\alpha b) + \left(\frac{4\alpha}{\pi}\right)^2 b \sum_{k=1,3,5}^{\infty} \frac{\sqrt{\beta_k}}{k^2\beta_k^2} \tanh\left(a\sqrt{\beta_k}\right)\right]^2 \tag{22}$$

Similar analysis yields a similar expression for the force produced by the other actuator

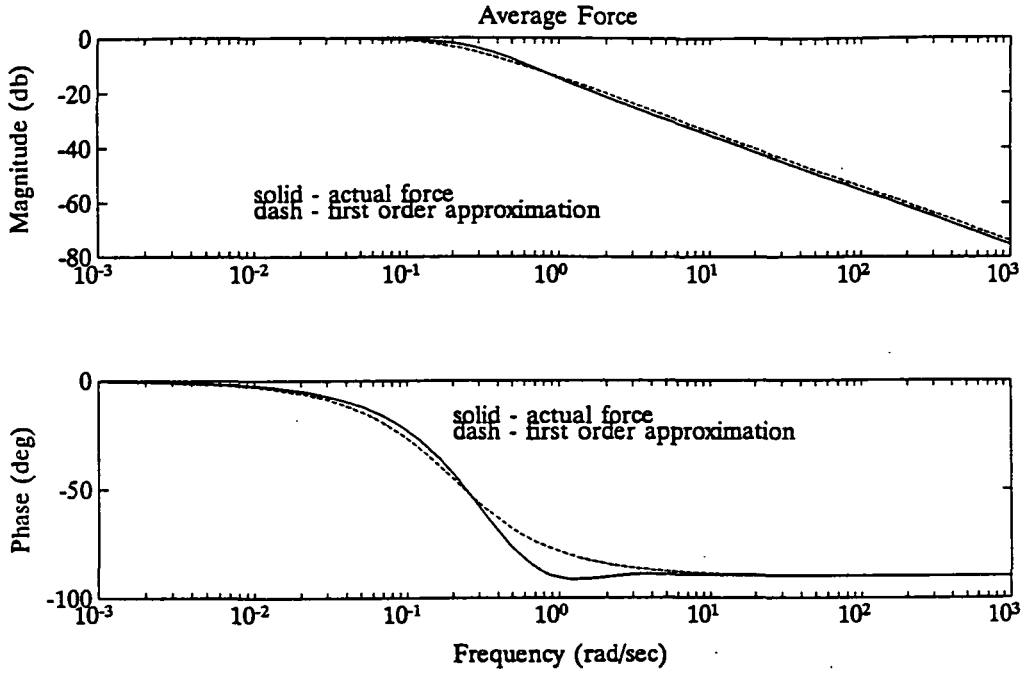

Figure 3: Normalized magnitude and phase of average electromagnetic force

$$F_{m2}(z,\omega) = \frac{\mu_0 N^2}{A}\left(\frac{I_2}{z_0 - z}\right)^2 \left[\frac{1}{\alpha} tanh(\alpha b) + \left(\frac{4\alpha}{\pi}\right)^2 b \sum_{k=1,3,5}^{\infty} \frac{\sqrt{\beta_k}}{k^2 \beta_k^2} \tanh\left(a\sqrt{\beta_k}\right)\right]^2 \qquad (23)$$

The normalized magnitude and phase of (22) are plotted in Fig. 3 and clearly show a first-order type response with a high frequency roll-off of approximately 20 db/decade and a phase lag at high frequencies of about 90 deg. The response of a first-order system of the form

$$\hat{F}(j\omega) = \frac{1}{1 + j\frac{\omega}{\omega_b}} \qquad (24)$$

is also plotted in Fig. 3. Comparison of the responses of the two functions indicates that, at least with respect to sinusoidal steady state conditions, the exact expression of (22) can be conveniently and accurately represented by the approximate expression of (24). While the break frequency ω_b is closely related to the $\sigma\mu$ product, an optimal value in a particular application is easily found numerically. The final forms of the frequency domain approximations for the magnetic forces are then

$$F_{m1}(j\omega) = \frac{\mu_0 N^2}{A}\left(\frac{I_1}{z_0 + z}\right)^2 \frac{1}{i + j\frac{\omega}{\omega_b}} \qquad (25)$$

and

$$F_{m2}(z\omega) = \frac{\mu_0 N^2}{A}\left(\frac{I_2}{z_0 - z}\right)^2 \frac{1}{i + j\frac{\omega}{\omega_b}} \tag{26}$$

While (25) and (26) are convenient frequency domain models of the response of magnetic force to sinusoidal steady state actuator current, it is also useful, for many design and analysis tools, to have equivalent time domain expressions. This can be accomplished with little justification, other than it produces an expression that appears to have the right form, by replacing $j\omega$ with s, holding i and z constant, and taking inverse Laplace transforms. The results are the first order differential equations

$$\frac{dF_{m1}}{dt} = -\omega_0 F_{m1} + \left(\frac{\mu_0 N^2 A \omega_0}{4}\right)\left(\frac{i_1}{z_0 + z}\right)^2 \tag{27}$$

and

$$\frac{dF_{m2}}{dt} = -\omega_0 F_{m2} + \left(\frac{\mu_0 N^2 A \omega_0}{4}\right)\left(\frac{i_2}{z_0 - z}\right)^2 \tag{28}$$

2.3 The Shaft

The objective of this section is to develop the equations of motion describing the dynamic response of the shaft to the forces imposed upon it. Referring to Fig. 1, application of Newton's second law gives rise to the following equations of motion

$$\frac{dz}{dt} = v \tag{29}$$

$$\frac{dv}{dt} = \frac{1}{M}\left[F_{m2} - F_{m1} - K_f v|v + F_d\right] \tag{30}$$

where v is the velocity of the shaft, M is its mass, K_f is a coefficient of viscous friction, and F_d is a disturbance force.

3 Conclusions and Recommendations

A new nonlinear dynamic model for use in the design and analysis of control systems for magnetic bearings has been presented. The time domain representation of the model is given by Equations (4), (5), (27), (28), (29), and (30). These equations are summarized below as a set of first order, nonlinear differential equations in state-variable form.

$$\frac{di_1}{dt} = -\frac{2(z_0 + z)Ri_1}{N^2\mu_0 A} + \frac{i_1 v}{z_0 + z} + \frac{2(z_0 + z)v_1}{N^2\mu_0 A} \tag{31}$$

$$\frac{di_2}{dt} = -\frac{2(z_0 - z)Ri_2}{N^2\mu_0 A} + \frac{i_2 v}{z_0 - z} + \frac{2(z_0 - z)v_2}{N^2\mu_0 A} \tag{32}$$

$$\frac{dF_{m1}}{dt} = -\omega_0 F_{m1} + \left(\frac{\mu_0 N^2 A \omega_0}{4}\right)\left(\frac{i_1}{z_0 + z}\right)^2 \tag{27}$$

$$\frac{dF_{m2}}{dt} = -\omega_0 F_{m2} + \left(\frac{\mu_0 N^2 A \omega_0}{4}\right)\left(\frac{i_2}{z_0 - z}\right)^2 \tag{28}$$

$$\frac{dz}{dt} = v \tag{29}$$

$$\frac{dz}{dt} = \frac{1}{M}\left[F_{m2} - F_{m1} - K_f v|v + F_d\right] \tag{30}$$

These six equations, and their linearized counterparts, form a convenient basis form magnetic bearing control system analysis and design. Research continues in two areas. First, to validate the proposed model with experimental data and second, to develop alternative control system designs compatible with VLSI implementation. Control system designs currently under investigation are based on the following approaches: a) classical frequency domain methods, b) modern H_2 and H_∞ methods, and c) neural network/fuzzy control methods. Results of these efforts will be published in future papers.

References

[1] J. J. Feeley, G. M. Niederauer, and D. J. Ahlstrom, "Fuzzy Control of Magnetic Bearings", NASA SERC Symposium on VLSI Design, 1991.

[2] F. Stolfi et. al., "Design and Fabrication of a Long-Life Stirling Cycle Cooler for Space Application", Phillips Laboratories report, March, 1983.

[3] Sadiku, M. N. O., "Elements of Electromagnetics", Saunders College Publishing, 1989.

[4] Stoll, R. L., "The Analysis of Eddy Currents", Clarendon Press, 1974.